4-26-2013

The Study of the Hidden Bearing Area: Comparison Between Flat and Corner Cushion Shock Test Performance

Chongyue Li

The Study of the Hidden Bearing Area: Comparison Between Flat and Corner Cushion Shock Test Performance

Master's Thesis

By

Chongyue Li

A Thesis Submitted in Partial Fulfillment of Requirements of the Master's Degree of Packaging Science

Department of Packaging Science

College of Applied Science and Technology

Rochester Institute of Technology

April 26, 2013

Committee Approval

Changfeng Ge, Ph.D., Associate Professor

Department of Packaging Science

Daniel Goodwin, Ph.D., Professor, Program Chair, Packaging Science

Department of Packaging Science

Deanna Jacobs, Packaging Graduate Program Chair

Department of Packaging Science

John Siy, Adjunct Professor

Department of Packaging Science

Abstract

Throughout history, cushioning material has been used widely in protective packaging design. Various cushioning materials included wood, paper, cloth, paperboard, molded pulp, plastic, and metal. However, the most popular and most effective since the last century is polymer plastic foam as protective cushioning packaging material. It has been comprehensively used for high-shock, compression, and vibration-sensitive products.

Over the past 60 years, scientists and engineers have a come a long way in both packaging-related academics and industries. A new series of testing standards was developed (ASTM D1596 and ASTM D4168) building up the cushion curve in terms of various foam materials, density, thickness, and drop height. Along with these standards came sophisticated engineering-cushion-design methods (Lansmont Six Step Method for Cushioned Package Development) that were developed to achieve the optimal and cost-effective transport solution.

However, due to the testing limitation of 90-degree shock impact, traditional cushion-curve methods lacked consideration of both the hidden bearing area in the corner-cushion design as well as the realistic and economical cushion material.

The following study, comparing the shock test performance between corner- and flat-cushion foam, qualitatively proved that the hidden bearing area does exist in the particular cushion geometry by conducting a dynamic acceleration-level response comparison between these two types of cushion design. It explored the possibility of a new experiment method for quantitatively formulating the hidden bearing area in the future. The shock test result recorded by accelerometers as G's response will provide packaging engineers with solid evidence of hidden bearing area existence, which needs to be considered for improving design accuracy and cost effectiveness by the traditional cushion curve. By conducting the measurement acceleration difference between the two types of cushion design, this study qualitatively proves that the hidden bearing area exists in this particular cushion geometry. This study explores the possibilities of new experiment methods that could be used as a guideline for protective cushioning design in both institute and industry for future use. Whatever the result may be, it will provide packaging engineers with solid evidence of the hidden bearing area's existence and improve both design accuracy and cost effectiveness.

Table of Contents

Abstract iii

Chapter 1 Introduction 1

Chapter 2 Cushion Material 4

2.1 Traditional cushion material and the materials of today 4
2.2 Why polymeric foam still cannot be replaced in certain locations 5

Chapter 3 Protective Packaging Development Process 7

3.1 Shock as hazard in transportation 7
3.2 Lansmont Six Steps of Protective Packaging Design Method 8

Chapter 4 Cushion Curve 10

4.1 Traditional Method of Cushion Curve: ASTM D1596 and ASTM D1468 10
4.2 How to design shock-resistance cushion using Cushion Curve 12

Chapter 5 Exploring Hidden Bearing Area 14

5.1 Motivation for exploring hidden bearing area 14
5.1 Hypothesis of hidden bearing area existence 16
5.2 Design of experiment 20
5.3 Analysis based on experimental results 23

Chapter 6 Conclusions 28

6.1 Experiment result proved existence of hidden bearing area 28
6.2 Quantitative difference ΔA between flat cushion and corner cushion structure 29
6.3 Importance of hidden bearing area study 29

References 31

Appendix A 32

Chapter 1 Introduction

For centuries people have been using various materials, such as wood, hay, fabric, paper, metal, and plastic, as cushion materials offering protection to our food, arms, and goods. After industrial polymerization was developed in the late 1800s, polymer plastic foams, such as Expanded Polystyrene (EPS), Polyurethane (PU), and Polyethylene (PE), gained their popularity fairly quickly. They were the most effective and reliable packaging cushion materials for high-shock-sensitive products, including large electronic equipment, optical electronic products, and military products [6].

The use of more sustainable packaging material has become increasingly popular over the past few decades, forcing engineers to become even more innovative than in the past. Modern cushion materials were developed and commercialized as an alternative to the original polymeric plastic foam. These new materials include molded pulp, thermoforming plastic, corrugated paperboard, and honeycomb board. However, polymeric plastic foam is still considered to be the most effective and reliable cushion material for products with high-shock sensitivity. It is superior in moisture resistance to high temperature and humidity during sea container transportation, as well as warehouse stacking durability, in comparison to paper- or wood-based cushion material. As discussed in Chapter 2, packaging engineers

recommended polymeric plastic foam above all others because of its multiple-shock performance. Polymeric plastic has an advanced shock resistance for complex transportation and rough-handling conditions.

Globalization is happening faster than ever, and, as a result, a large percentage of the U.S. market is purchased, manufactured, packaged, and distributed worldwide. The majority of our commodities are even transported across the globe, increasing the need for sturdy and reliable packaging.

In Chapters 3 and 4, it is not only important to achieve the goal of optimizing usage of material but also to control both the cushion thickness and the overall package dimension. This has now become a critical objective for both a company's profitability and environmental sustainability.

In Chapter 5, given the brief design guidance by traditional foam-cushioning-curve methodologies ASTM D1596 – 97(2011) "*Standard Test Method for Dynamic Shock Cushioning Characteristics of Packaging Material"* [2] and ASTM D4168 - 95(2008)e1 *"Standard Test Methods for Transmitted Shock Characteristics of Foam-in-Place Cushioning Materials"* [3], a hypothesis of hidden bearing area existed in certain geometries of cushion design (corner and edge), which may have had a negative influence on both accuracy and predictability. A study that compared G's response to

flat- and corner-cushion designs was then initiated and comprised of three method design experiments. One was selected by the shock tester and eventually performed. Finally, data analysis from the test results showed that there was a horizontal shift between the rebuilt cushion curve of the flat and corner designs, proving the hypothesis of the existing hidden bearing area.

The meaning of this study and the significance behind it can be found in Chapter 6. For packaging professionals looking to broaden their research, experimental methodologies and further possibilities are provided for discussion on this topic.

Chapter 2 Cushion Material

2.1 Traditional cushion material and the materials of today

Before polymeric plastic was discovered and compounded in the 1800s, people had been using a variety of natural cushion materials, such as wood, hay, cotton, fabric, and paper packing, and securing anything fragile [1].

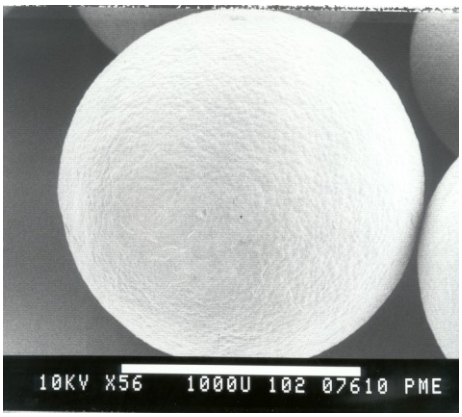

Figure 1EPS cell

Popular polymeric plastic foams, such as Polyethylene (PE) in Figure 1, Expanded Polystyrene (EPS) in Figure 2, and Polyurethane (PU), Polypropylene (PP), and inter-polymer (PS/PE), began to be used as protective packaging material since Dow Chemical first commercially manufactured Expanded Polystyrene in 1954 [2]. Since then consumers have seen, touched, recycled, and/or discarded a great percentage of plastic foam used as protective-cushion-packaging material, for everything from auto parts to food. Because of the relatively new concern about our environment, packaging engineers around the world have begun to design "greener"


Figure 2 PE cell

packaging—the more reusable and recyclable, the better. Many companies have started to use alternative cushion materials, as molded pulp, corrugated paperboard, honeycomb board, and plastic air pillows have replaced polymeric foam in many areas due to their cost effective, biodegradable, and easily recyclable nature. For example, large photography companies like Nikon have started to package even their most expensive DSLRs in molded pulp and corrugated board structure; in the 1980s hardly anything was used except EPS. Only time will tell if polymeric foam will become extinct in the near future [5].

2.2 Why polymeric foam still cannot be replaced in certain locations

First, as stated previously, polymeric foam has superior durability in cross-geometric transportation, whether domestic or international. Figure 3 portrays the temperature and humidity data that was captured in early September 2012 from a 53-foot truck trailer on its journey from Mexico to Memphis, TN. The products in this study were Honeywell Air Purifiers, some packaged with EPS and others with molded pulp, both in 45ECT BC double-wall retail packages. Engineers and technicians met the truck as it arrived on the dock to evaluate the condition of the packages. They found that the air purifiers packaged in molded pulp showed more levels of displacement and degradation than those packaged in EPS. It is interesting because this phenomenon typically only happens in the dry, cool

conditions of the winter season. A similar situation happened when packaging of the same caliber was stacked and stored in a warehouse for 6–18 months.

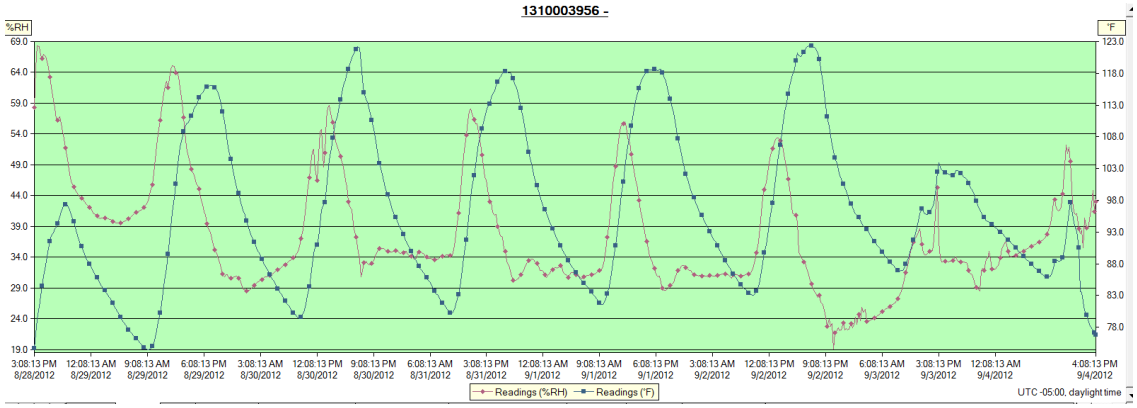

Figure 3 Environmental data from Mexico to Memphis, TN

Secondly, this collected data only reinforces that polymeric foam is still the most reliable form of cushioning in terms of G's response. Scientists continue to work on strengthening the pulp-based curve design, but because of the nature of the material itself, it is subject to different temperature and moisture levels.

Thus, polymeric foam still cannot be replaced in many locations around the world, since alternatives such as molded-paper pulp become defective in extreme humidity and moisture. Many products with high-shock sensitivity need superior protection and cannot be compromised by a weak packaging material. Discussions about whether or not polymeric foam should be used at optimum volumes and sizes have become a critical topic and will continue to be debated for years to come.

Chapter 3 Protective Packaging Development Process

3.1 Shock as hazard in transportation

In today's highly industrialized world, commodities are manufactured and distributed in an increasingly complicated way. In order to reach the consumer, the product is usually manufactured, assembled, and packaged overseas, then transported to a warehouse, and finally distributed to a company before the consumer even has a chance to view it. The retail packages are placed in a master carton, which is then placed in an outer shipper with others of its kind. All outer shippers are put onto a sea container to then be shipped by rail and truck to a warehouse. Depending on where the goods are being delivered, they are then either delivered to a retailer's distribution center or a small parcel shipment company, such as FedEx or UPS. Shock is one the major transportation hazards during the entire complex logistic process, along with compression, vibration, temperature, moisture, chemicals, and electronic magnetic interference [1].

Package Weight	Type of Handling	Suggested Drop Test Heights
0-20 lbs	one man throwing	42 inches
20-50 lbs	one man throwing	36 inches
50-250 lbs	two men carrying	30 inches
250-500 lbs	light equipment	25 inches
500-1000 lbs	light equipment	18 inches
over 1000 lbs	heavy equipment	12 inches

Figure 4 ISTA drop height chart courtesy of ISTA

According to an established ISTA study as shown in Figure 4, shock from various transportation methods are quantified in different severity levels in terms of weight and dimension. The transportation methods compared are handling, lifting, and equipment lifting. This study provided a valuable guideline for packaging engineers when analyzing and evaluating hazards during the distribution process. It also added insight when setting up appropriated packaging-testing criteria, making it easier to gather data on future projects [7].

3.2 Lansmont Six Steps of Protective Packaging Design Method

Safety and cost effectiveness are two factors that packaging industries are always striving to improve. Scientists and engineers alike put tremendous effort in developing design methodologies to enhance them. As one of the most remarkable achievements, Lansmont “Six Step Method for Cushioned Package Development”

became the most prevalent and useful cushion-package design, a reliable and well-tested method in the current packaging academy and industry. With guidance from its established practice, packaging engineers could control the balance of damage impact from inadequate package versus cost impact from over pack and less container-cube efficiency as much as possible [8].

Chapter 4 Cushion Curve

4.1 Traditional Method of Cushion Curve: ASTM D1596 and ASTM D1468

Traditionally cushion curves can be tested by two approaches: the guided platen method (GPM) as ASTM D 1596 *Standard Test Method for Shock Absorbing Characteristics of Package Cushioning Materials*, as shown in Figure 5, and the enclosed test block (ETB) method used as ASTM D 4168 *Standard Test Methods for Transmitted Shock Characteristics of Foam-in-Place Cushioning Materials,* as shown in Figure 6. In the first method, ASTM D 1596, the polymeric foam is prepared in a certain way, measuring to 4" x 4". After this preparation, it is placed on a massive platform and dropped from a predetermined height. As it falls, the peak acceleration value is captured and recorded by a specific program. Density and thickness, respectively, of cushion foam can be varied in testing for building response; drop height and various masses can be adjustable in order to perform different static loadings. As shown in Figures 5 and 6, a standard cushion tester and one 2.2 pcf polyethylene, 12-inch impact cushion curve is tested by the ASTM D 1596 approach. Because this test method allows for the assumption that the cushion has to be a certain size (4" x 4"), it is at a great disadvantage in comparison to the ASTM D 4168. While in theory it works, in reality the cushion cavity always has to accompany the

product industrial design [2].

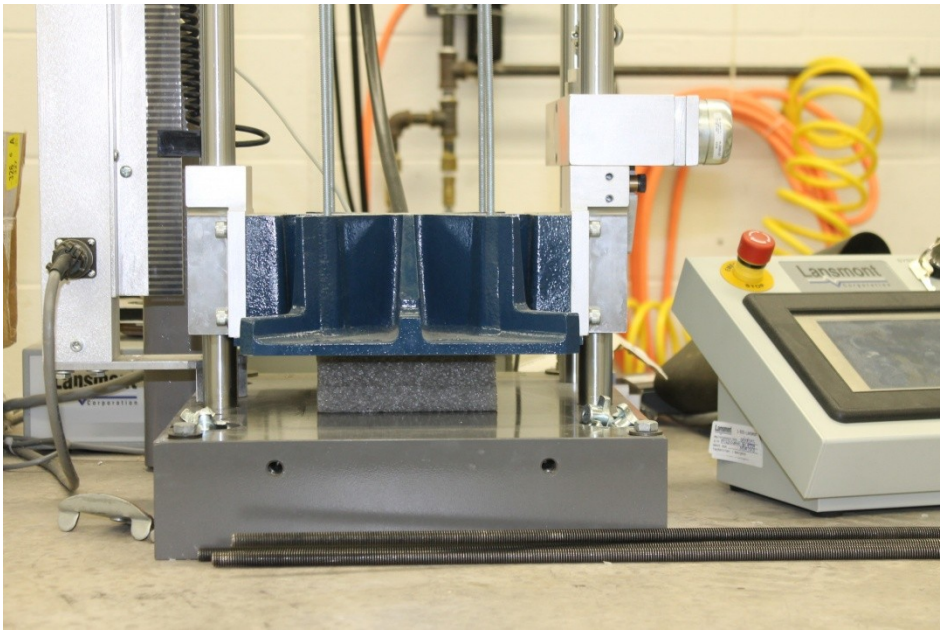

Figure 5 The guided platen method (GPM) ASTM D1596

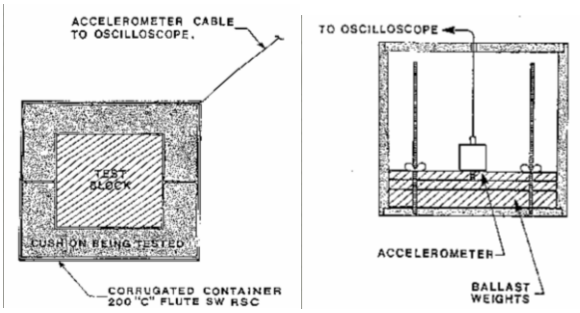

Figure 6 The enclosed test block (ETB) ASTM D4168

ASTM D 4168, also known as “foam in place” testing, has taken into consideration the practicality of reality. This test standard was developed specifically for

improving the accuracy of foam-cushion properties. You can also see in Figure 6 above that the adjustable mass and sensor-recording-peak-acceleration value is placed in a foam-in-place system, and the shock test is performed on the whole system rather than separately. The second test method is more commonly used, mostly due to how much closer it is to how the product would be placed in a cushioned package during actual manufacturing. However, it does still lack a few key components of the real world. It does not take into account that both material consumption and static loading need to be adjustable in order to perform the highest-quality shock absorption [3].

4.2 How to design shock-resistance cushion using Cushion Curve

Product	Description	G's Level
Extremely Fragile	Aircraft altimeters, gyroscopes, items with delicate mechanical alignments	15-25 g's
Very Delicate	Medical diagnostics apparatus, X-ray equipment	25-40 g's
Delicate	Display terminals, printers, test instruments, hard disk drives	40-60 g's
Moderately Delicate	Stereo and television receivers, floppy disk drives	60-85 g's
Moderately Rugged	Household appliances, furniture	85-115 g's
Rugged	Table saws, sewing machines, machine tools	115 g's +

Figure 7 Product Fragility Level courtesy of ISTA

Once the distribution environment (drop height), product-fragility level (the G's requirement), and the best applicable cushion-foam density is known, the equation for the most effective cushion-bearing area (A) is as follows:

$$Static\ Stress(psi) = \frac{Weight\ (lbs)}{Bearing\ Area\ (inch^2)}$$

$$\sigma = \frac{M}{A}, \quad A = \frac{M}{\delta}\ (1)$$

By understanding the cushion curve, known by the optimized G's value that corresponds with the static loading (σ) and total mass of the product (M), the calculation for the optimized-bearing area becomes available (A) (1).

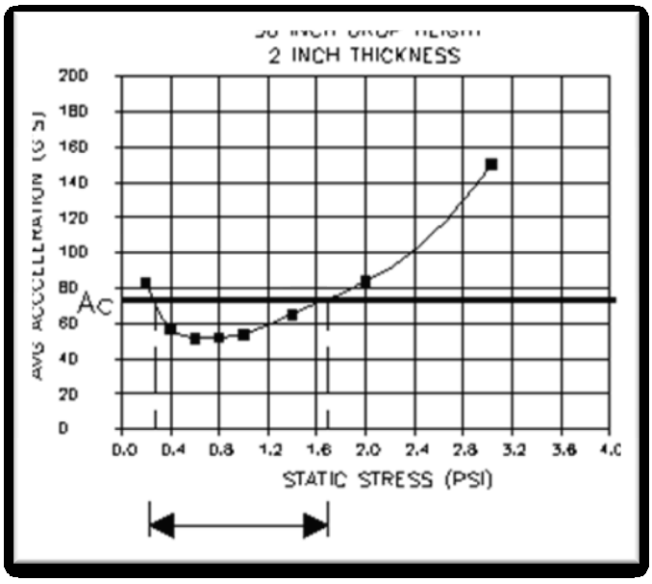

Figure 8 Design by cushion curve

Chapter 5 Exploring Hidden Bearing Area

5.1 Motivation for exploring hidden bearing area

As a packaging engineer, I primarily develop, design, and test protective packaging systems for consumer electronics products. During years of cushion-package-design experience, I sometimes have packaging performance issues during shock and vibration validation tests, when I tried designing PE and/or EPS foam cushion under the guideline of the cushion curve provided by manufacturers. In detail, cushion sets are designed at optimum foam thickness; static stress and bearing area, however, do not always perform at what was indicated by the corporate cushion curve in terms of peak acceleration value. In some cases, the actual peak acceleration measured through drop testing exceeds the acceptable product-fragility level, which somehow causes product failure in functionality and/or appearance. In order to

Figure 10 Purification Unit

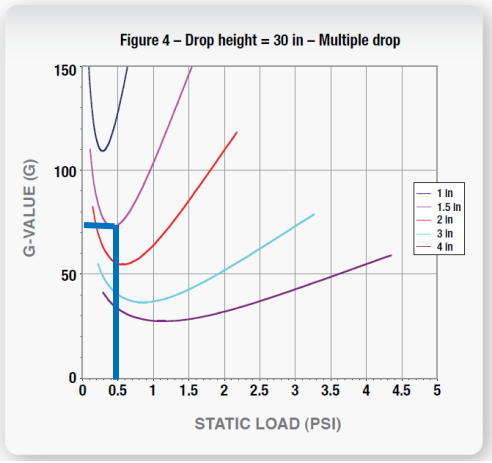

Figure 9 1.8pcf foam courtesy of Sealed Air

avoid this scenario, I have to utilize extra cushion thickness providing additional protection, which is not preferable because it not only increases the usage of cushion material and secondary packaging material (such as corrugated board), but it also means higher freight costs due to the reduced pallet and container quantity.

Using one of my previous product-packaging designs as a good example, with a purification unit weight of 14.5 lbs and the fragility level at 85 G's, the product was drop tested at height of 20 inches according to ISTA 1A procedure. Initially, 1.8 pcf, 1.5 inch thickness PE foam was selected by the guideline of the existing cushion curve. The estimated peak acceleration value was supposed to be 75 G's when the optimum static stress of 0.4 psi was chosen. However, the product was damaged and the actual measured acceleration value was over 100 G's during the preliminary packaging drop test. Eventually, cushion thickness was upgraded from 1.5 inches to 2 inches in order to provide adequate protection to the product. A negative impact to the overall distribution process is not only using more material but also shipping less quantity in the container. In a 40-ft high cube sea container, the actual quantity is 644 (2" cushion) versus the estimated 736 (1.5" cushion). As a result, the shipping cost increase is 14%.

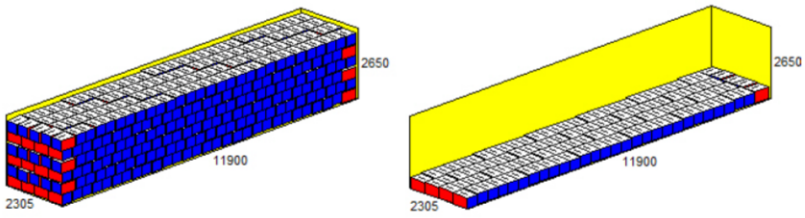

Figure 11 40ft HQ container loading

5.1 Hypothesis of hidden bearing area existence

As discussed in Chapter 4, the bearing area theoretically is the area where the mass (product) comes into contact along the impact direction. The cushion shape is hardly designed as a perfect 90 degree angled block; in fact, it usually comes in the shape of a corner pad, edge pad, and/or edge cap, as shown in Figures 9 and 10. These shapes actually offer the most potential, as there may be some bearing area hidden inside [4].

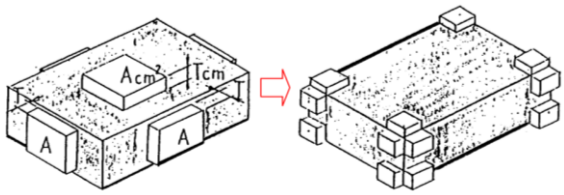

Figure 12 Corner cap

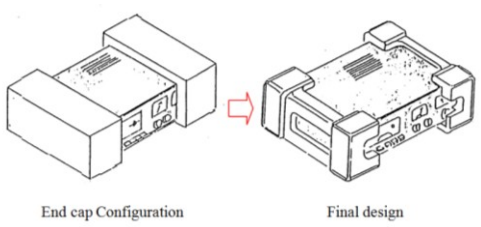

Figure 13 End cap

The significant difference between a flat cushion and a corner cushion is that the corner cushion has tensile strains presented within the area between product edge and the inner side of the cushion. As shown in Figures 11 and 12, though major compression stress is applied on the vertical direction, part of the inner-corner cushion is still involved with the reaction; refer to FEA simulation for a corner cushioning under a vertical dynamic stress done by Mills and Masso-Moreo [6].

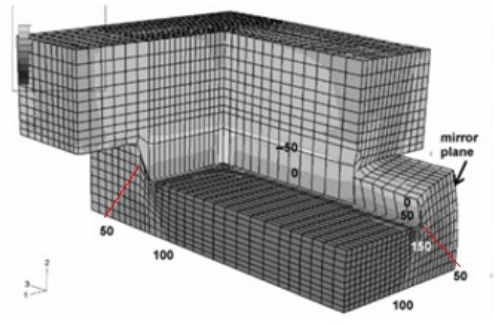

Figure 14 The FEA predicted deformation of the corner PE cushioning under the vertical dynamic compression

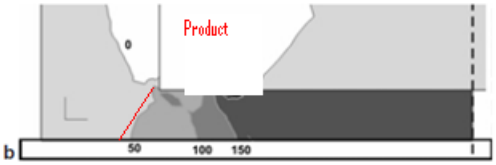

Figure 15 The FEA predicted deformation of the edge PE cushioning under the vertical dynamic compression [6]

In order to build a corner-cushion curve utilizing the traditional cushion curve developed by the GPM (ASTM D1596) method, foam blocks need to be a certain thickness and square shape. The corner-cushion structure was bridged as a flat-block cushion (cushion B, bridge cushion) with identical thickness and extra surface, which represent a hidden bearing area in the corner cushion.

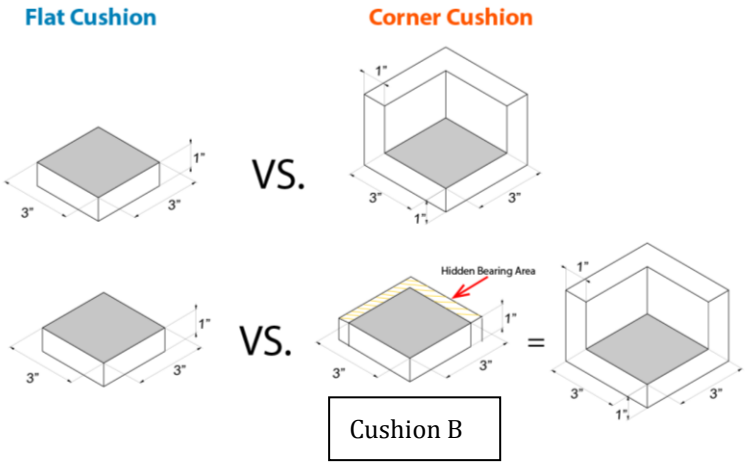

Figure 16 Flat cushion vs. Corner cushion

As in Figure 14, the existing flat curve is shown in blue. Because

$Ab = Af + \Delta A$ (ΔA is hidden bearing area)

Known that, $\sigma_f = \frac{M}{Af}, and\ \sigma_b = \frac{M}{Ab}$

$$\Delta A = Ab - Af = \frac{M}{\sigma_b} - \frac{M}{\sigma_f} \ (2)$$

Assuming hidden bearing area (ΔA) exists and ΔA>0, that $\frac{M}{\sigma_b} - \frac{M}{\sigma_f} > 0$

M>0

So, $\frac{M}{\sigma_b} > \frac{M}{\sigma_f}, then\ \sigma_b < \sigma_f.$

$$\Delta\sigma = \sigma_f - \sigma_b \ (3)$$

In the GPM (ASTM D1596) method, G's performance is correlated with σ at a certain cushion size. Therefore, in order to generate equivalent B cushion (corner cushion) to G's response value, we should use a reduced-static-stress value on the flat-cushion curve, shown as green and blue dashed lines in Figure 13. The B-cushion curve should have a right-direction shift rather than an existing flat-cushion curve; the value of shift on static stress is equal to Δσ.

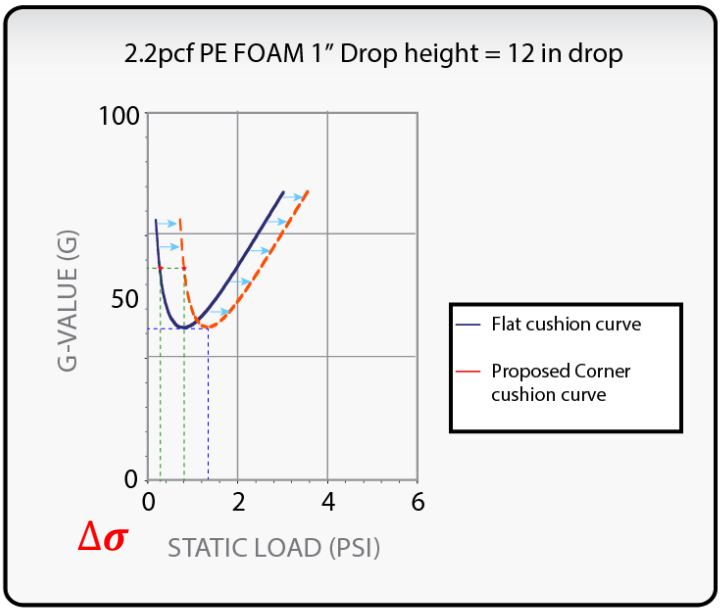

Figure 17 Hidden bearing area courtesy of Sealed Air

5.2 Design of experiment

Figure 18 Flat cushion in experiment

Figure 19 Corner cushion in experiment

Extruded polyethylene foam at a 1-inch thickness and 2.2 pcf density was selected as a popular cushion in consumer electronics since it is inexpensive and easily prototyped. Figures 15 and 16 are photographs of both a 3" x 3" flat cushion and a 3" x 3" corner cushion with 1-inch wall thickness provided by Orcon Industry. After samples are cut by an ESKO Kongsberg Cutting Table to achieve sample quality and reduce the variables or prototyping, the corner cushions are heat glued with a manufacturing foam heat gun specifically sold for this purpose. With four cushions per set, over 150 sets of each design are prepared for testing this way. The weight of the smooth, solid steel varies from 2-53 lbs, all professionally prepared by Eastman Kodak Company and RIT Dynamic Laboratory, which were both a great help. The wood frame and the steel rod fixture keep both the cushions and their weight in the intended position.

In total, there are three proposed experimental methods: the cushion test as ASTM D 1596, the drop test, and the shock test. As a first attempt, the exact cushion tester as ASTM D 1596 was proposed for testing. Because it was used for the traditional

cushion curve that minimizes variables between different testing equipment, it made for an ideal initial testing method. However, several concerns were raised: 1) it is difficult to control whether or not the steel mass will land on the entire bearing area of cushion that is placed on the base and particularly unrealistic to control whether or not it will hit the corner cushion; and 2) because the main objective of the experiment is to prove that the hidden bearing area exists in real-world packaging design, the test needs to be designed as closely as possible to what the product will be going through during manufacturing.

The second experiment is done by the drop tester and is intended to simulate product free falls during mishandling. The main problem, however, is that it needs to be packed in a box. Whether it is a corrugated board (as thin as E-flute) or paperboard, the variable weight can cause unexpected errors in the data.

In the final experiment, the shock tester was selected as the final solution. Not only does it have highly controllable programs, but it also has a flat-steel plate that is the most appropriate for mounting cushion samples and fixtures, ensuring even shock impact.

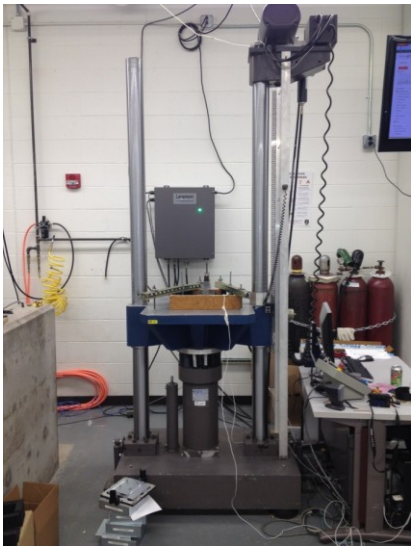

Figure 20 Shock Tester

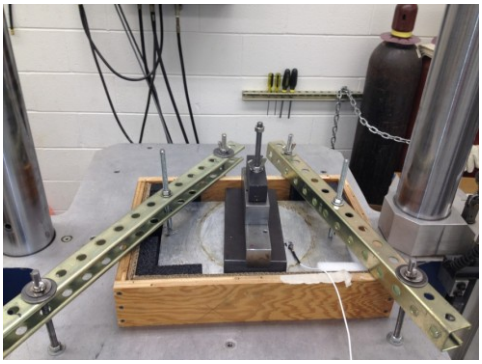

Figure 21 Weight, sensor, and fixture

5.3 Analysis based on experimental results

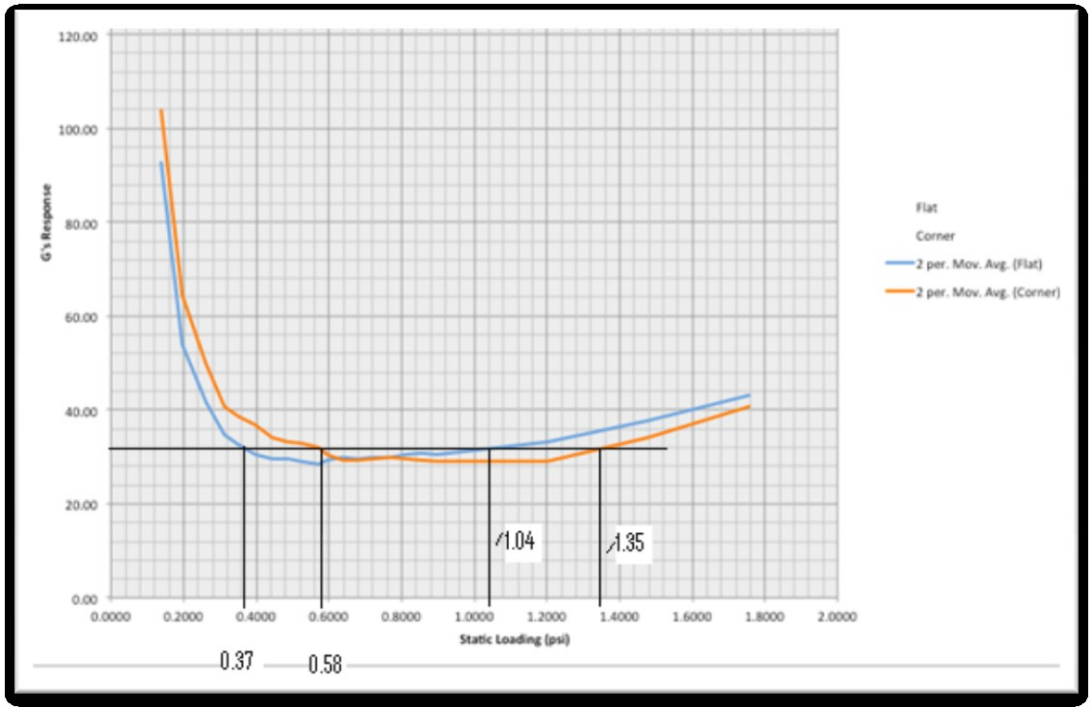

Figure 22 Flat and corner curve from experiment

Because of the close dimension between the flat- and corner-foam cushions, there is a slight right shift from the flat-cushion curve to the corner-cushion curve, as

hypothesized in Chapter 5.1. In detail, the flat cushion reached its minimal G's level of 28.25G's at a static loading of 0.5703psi, whereas the corner-cushion curve held its lowest G's level of 29.02G's at a greater static loading of 0.6394psi. Regarding its minimal G-value difference, the static loading has a shift of 0.0691psi, which is equivalent to an 11% bearing area increase [4].

As illustrated in Figures 19 and 20, there are three regions segmented by two-cushion curves in G's level response in terms of static loading stress.

Region	Static Loading Stress	G's Level Response
Ⅰ	0.18-0.62psi	Corner cushion G-value generaly higher than flat cushion
Ⅱ	0.62-0.76psi	Corner cushion and flat cushion G-value generaly keep same value
Ⅲ	0.76-1.76psi	Corner cushion G-value generaly lower than flat cushion

Figure 23 Three regions

Also from the experiment, the hidden bearing area value (percentage) varies with regard to different levels of static stress, as shown in Figures 21 and Figure 22. Cushion curves are divided into three sections according to static stress levels:

1. Zone I: under optimum static loading
2. Optimum point: the lowest G's value
3. Zone II: over optimum static loading

$$\frac{\Delta A}{Af} = \frac{(Ac - Af)}{Af} = \frac{\left(\frac{M}{\sigma_c} - \frac{M}{\sigma_f}\right)}{Af} = \frac{\Delta\sigma}{\sigma_c} \cdot 100\% \quad (4)$$

In Zone I, ΔA keeps increasing along with static stress σ and reaches its peak of 56.67% of Af, then decreases gradually to 10% in Zone II. This result is significant in that neither ΔA nor Δσ stay the same for different shock levels. The static stress value chosen by the packaging designer around the optimum point on the cushion curve, since it is the first and best solution, might miscalculate the hidden bearing area (ΔA) by as much as 56.67%.

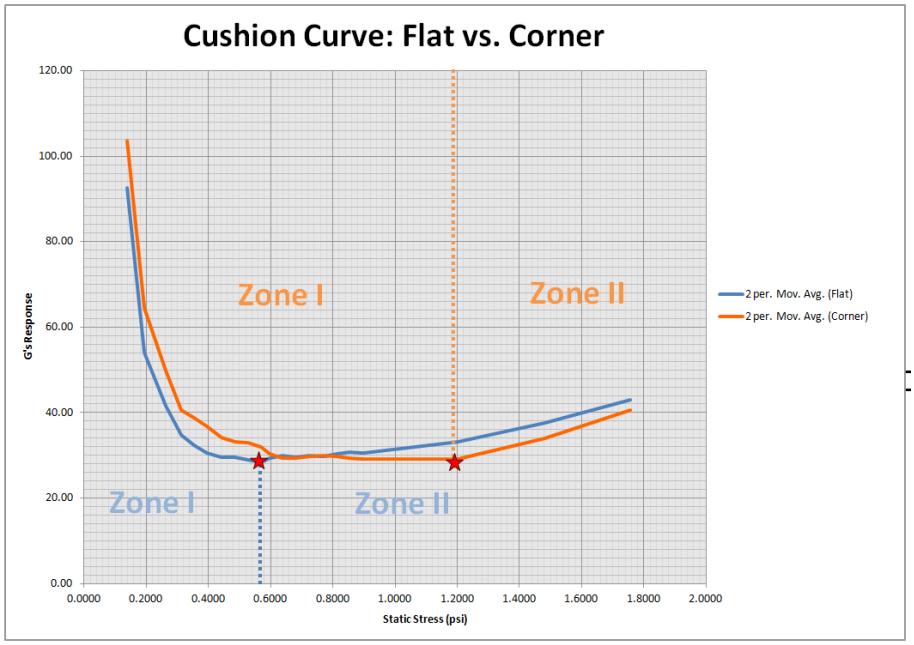

Figure 24 Zone I, Optimum point, and Zone II

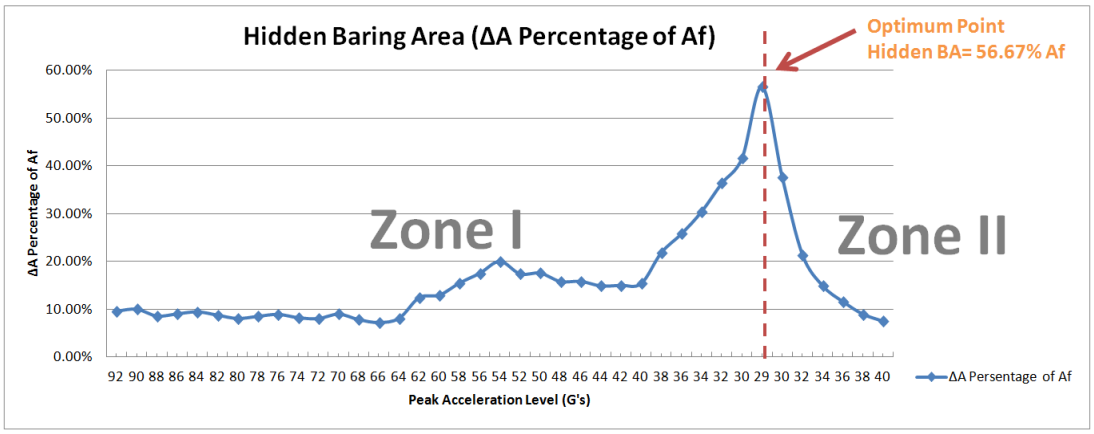

Figure 25 Hidden bearing area ΔA percentage

For example, the tested cushion curves of both the flat and corner foam are shown as black horizontal lines, assuming that a cushioning package with a fragility level of 32G's will need to be developed. There are a total of four intersections between the black lines and the two cushion curves. In the right portion, the horizontal line meets the flat-cushion curve at a static stress of 1.04psi and a corner cushion at 1.35psi. Based on our calculation in (1), the difference of bearing areas between the two intersections will be shown in the calculation below:

$$\Delta A = (\,Af - Ac) = \left(\frac{M}{1.04} - \frac{M}{1.35}\right) = 0.22\ M; \qquad (5)$$

M = Product Weight

Compared to the original bearing area Af, the increased bearing area in percentage

can also be calculated as follows:

Bearing area increase in percentage = $\frac{\Delta A}{Af} = \frac{0.22\ M}{M/1.08} \cdot 100\% = 23.8\%$ (6)

Based on the existing cushioning curve in the industry that measured from flat to geometry, the 23.8% of the bearing area should be taken into consideration when designing a cushioned package using a corner configuration. Indeed, the hidden bearing area existed in the corner cushioning that provides more bearing area than a flat cushioning with the same bearing area to a product. The hidden bearing area existed in the corner cushioning, providing more bearing area than a flat cushioning with the same bearing area. The equation can be calculated as follows:

$$\Delta A = (\ Af - Ac) = \left(\frac{M}{0.37} - \frac{M}{0.58}\right) = 0.98\ M \qquad (7)$$

M= Product Weight

Compared with the original bearing area (Af), the increased bearing percentage can also be calculated as follows:

Hidden bearing area in percentage = $\frac{\Delta A}{Af} = \frac{0.98\ M}{M/0.37} \cdot 100\% = 36.3\ \%$ (8)

Chapter 6 Conclusions

I discovered from the shock test study that flat- and corner-foam cushions have very similar geometry. The results of the experiment particularly proved that the hidden bearing area has become a factor that cannot be ignored and, therefore, needs to be taken into consideration during the cushion-design process.

6.1 Experiment result proved existence of hidden bearing area

From the cushion curve built by the experimental result, we can clearly see there is a right shift on the corner-cushion-curve base on the flat-cushion curve, which proved the Chapter 4 “Hypothesis of hidden bearing area” quantatively. Both curves reached their optimum point at around 29 G’s at their optimum static stress levels, respectively, which showed the evidence that the corner cushion will not influence overall cushion thickness; it only affects static stress due to its additional hidden bearing area. In other words, if you cannot use the flat-cushion curve to meet the minimal G’s level requirement when doing packaging design, you will not get any extra protection from the thickness from corner-cushion structure.

6.2 Quantitative difference ΔA between flat cushion and corner cushion structure

From experimental results, ΔA variation is not simply a fixed value through all of the static stress ranges. It actually varied from 9.68%, gradually increasing with increasing static stress σ in Zone I until it reached its greatest of 56.67% at the curve's optimum point; then it started decreasing gradually to 7.55% in Zone II. In this scenario, the corner cushion from the experiment is different than the dashed corner-cushion curve proposed in Chapter 4, because it is a complex-variable value rather than a fixed value. In addition, it reached its most significant value of as much as 56.67% at the optimum point, which normally is chosen as the best performance and most cost-effective solution.

6.3 Importance of hidden bearing area study

Disregarding the difference between the flat and corner cushion may lead to high risk or even damage to product due to inadequate protection provided by the package. Additional bearing areas hidden inside the corner cushion, as proved by the study, will consequently cause the decrease of static stress σ, assuming there is no weight change. This static stress decreases, especially in Zone II; under optimum static stress it might provide the packaging designer with incorrect corresponding acceleration data and might increase the risk of damage if the actual peak

acceleration value equals or exceeds the minimum product-fragility requirement.

For example, in Figure 23, 50 G's is the product-fragility requirement, and the cushion design is a corner structure. Targeting the flat-cushion optimum point (static stress= 0.8 psi) seems to offer the best result at about 40 G's (target G's value). However, the peak acceleration value of the corner cushion will be as high as 60 G's, which is significantly over the product minimum requirement of 50 G's. The product will be damaged by disregarding the hidden bearing area in the corner cushion.

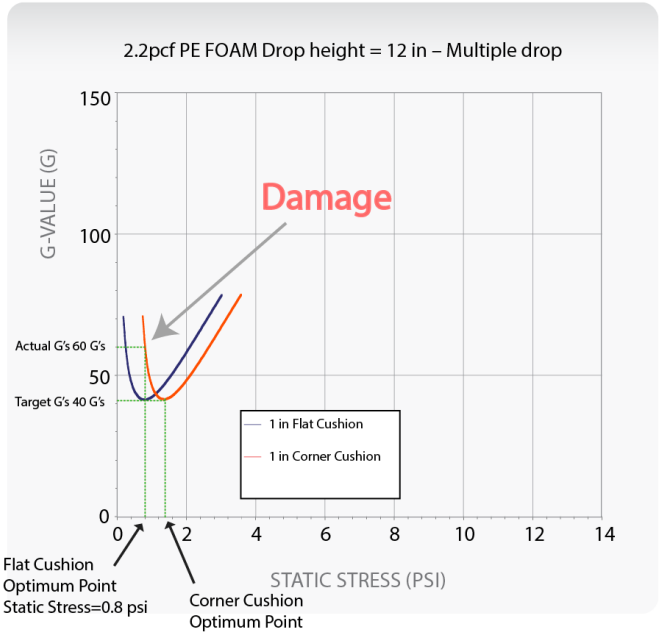

Figure 26 Incorrect calculation causes damage

References

[1] Daniel, G., & Dennis, Y. (2011). *Protective Packaging for Distribution: Design and Development.* Lancaster, PA: DEStech Publications, Inc. ISBN: 978-1-60595-001-3.

[2] ASTM Standard D1596-97. (2011). *Specification Standard Test Method for Dynamic Shock Cushioning Characteristics of Packaging Material,* ASTM International, West Conshohocken, PA. DOI: 10.1520/D1596-97R11, www.astm.org

[3] ASTM Standard D4168-95. (2008). *Standard Test Methods for Transmitted Shock Characteristics of Foam-in-Place Cushioning Materials,* ASTM International, West Conshohocken, PA. DOI: 10.1520/D4168-95R08E01, www.astm.org

[4] Changfeng, G., Chongyue, L., Daniel, G., Thomas, K. & Haoqi, H. (2013). *A comparison study in cushion curves between a flat cushioning and a corner cushioning.* Rochester, NY. ISTA's TransPack Forum.

[5] Mills, N.J. (2007). *Polymer Foams Handbook.* ISBN-13: 978-0-7506-8069-1.

[6] Mills, N., & Masso-Moreu, Y. (2005). *Finite element analysis (FEA) applied to polyethylene foam cushions in package drop tests,* Packaging Technology and Science, Volume 18, issue 1 (January/February 2005), pp. 29 - 38. DOI: 10.1002/pts.676.

[7] International Safe Transit Association. (2013). *ISTA Resource Book.* Lansing, MI.

[8] Lansmont Corporation. (1988). *Six Step Method For Cushioned Package Development.* http://www.lansmont.com/SixStep/

[9] Stupak P.R. & Donovan J.A. (1992). *Load spreading and polymeric foam energy absorber design,* SAE Trans. 101, Section 6, pp. 263-269.

Appendix A

Figure 1EPS cell 4
Figure 2 PE cell 4
Figure 3 Environmental data from Mexico to Memphis, TN 6
Figure 4 ISTA drop height chart courtesy of ISTA 8
Figure 5 The guided platen method (GPM) ASTM D1596 11
Figure 6 The enclosed test block (ETB) ASTM D4168 11
Figure 7 Product Fragility Level courtesy of ISTA 12
Figure 8 Design by cushion curve 13
Figure 9 1.8pcf foam courtesy of Sealed Air 14
Figure 10 Purification Unit 14
Figure 11 40ft HQ container loading 16
Figure 12 Corner cap 16
Figure 13 End cap 17
Figure 14 The FEA predicted deformation of the corner PE cushioning under the vertical dynamic compression 17
Figure 15 The FEA predicted deformation of the edge PE cushioning under the vertical dynamic compression [6] 18
Figure 16 Flat cushion vs. Corner cushion 18
Figure 17 Hidden bearing area courtesy of Sealed Air 20
Figure 18 Flat cushion in experiment 20
Figure 19 Corner cushion in experiment 21
Figure 20 Shock Tester 22
Figure 22 Flat and corner curve from experiment 23
Figure 21 Weight, sensor, and fixture 23
Figure 23 Three regions 24
Figure 24 Zone I, Optimum point, and Zone II 25
Figure 25 Hidden bearing area ΔA percentage 26
Figure 26 Incorrect calculation causes damage 30

Flat Cushion (h/d=12) 1st Shock						
Measured Value						
σ- Static Loading (psi)	1st G's	2nd G's	3rd G's	4th G's	5th G's	2-5 Avg.
0.0556	124.32	122.76	120.86	123.92	124.03	122.89
0.1389	60.96	61.02	60.90	60.62	61.82	61.09
0.1944	47.04	48.73	51.06	51.38	52.62	50.95
0.2619	36.33	39.23	40.34	40.78	41.58	40.48
0.3125	33.18	36.11	37.17	38.06	38.35	37.42
0.3531	31.71	34.96	36.17	37.31	38.55	36.75
0.3958	29.33	33.27	35.17	36.10	36.68	35.31
0.4433	29.82	34.05	35.81	37.59	37.27	36.18
0.4861	29.10	33.35	35.82	37.12	37.31	35.90
0.5267	28.61	33.37	35.59	36.25	37.39	35.65
0.5703	28.25	33.65	35.29	38.01	38.59	36.39
0.5967	30.60	36.54	38.94	40.42	41.44	39.34
0.6394	29.23	36.50	38.21	38.99	39.65	38.34
0.6800	29.70	37.35	40.45	40.36	43.74	40.48
0.7228	30.07	37.94	40.36		43.11	40.47
0.7703	29.58	38.20		43.29	44.06	41.85
0.8131	31.18	40.15	43.51	43.55	49.17	44.10
0.8536	30.42	41.28	45.93	47.10	48.05	45.59
0.8964	30.68	43.93	48.36	45.66	52.76	47.68
1.2014	35.55	47.04	51.98	53.30	51.50	50.96
1.4792	39.55	52.61	56.45	59.52	59.73	57.08
1.7569	46.59					

Corner Cushion(h/d=12) 1st Shock						
Measured Value						
	1st G's	2nd G's	3rd G's	4th G's	5th G's	2-5 Avg.
	135.77	138.68	135.17	134.00	133.10	135.24
	71.66	74.80	73.37	73.47	73.62	73.82
	57.25	60.50	61.73	61.59	62.78	61.65
	42.28	45.38	48.43	49.74	50.34	48.47
	39.03	42.23	46.06	47.66	48.50	46.11
	38.39	41.60	44.69	45.91	46.81	44.75
	35.03	39.37	43.36	44.74	46.02	43.37
	33.33	37.85	45.73	43.66	44.60	42.96
	32.87	37.01	40.88	41.87	43.18	40.74
	32.92	35.93	40.97	42.96	44.91	41.19
	31.01	36.76	40.33	42.86	44.08	41.01
	29.67	36.71	40.68	41.85	42.65	40.47
	29.02	32.93	38.94	42.06	43.96	39.47
	29.64	36.94	42.59	45.20	47.47	43.05
	29.68	35.70	41.36	44.25	46.35	41.92
	30.06	37.46	45.66	47.67	49.52	45.08
	29.25	40.15	45.01	47.69	50.18	45.76
		42.95	46.87	49.56	51.25	47.66
	29.07	39.75	44.74	47.26	48.99	45.19
	29.13	47.68	54.67	59.77	61.62	55.94
	38.93	58.56	68.27		76.34	67.72
	42.20					

ΔA Persentage of Af					
	G's	Flat Static Stress	Corner Static Stress	Δstatic stress	ΔA Persentage of Af
Zone I	92	0.140	0.155	0.015	9.68%
	90	0.143	0.159	0.016	10.06%
	88	0.148	0.162	0.014	8.64%
	86	0.150	0.165	0.015	9.09%
	84	0.152	0.168	0.016	9.52%
	82	0.155	0.170	0.015	8.82%
	80	0.158	0.172	0.014	8.14%
	78	0.160	0.175	0.015	8.57%
	76	0.162	0.178	0.016	8.99%
	74	0.166	0.181	0.015	8.29%
	72	0.170	0.185	0.015	8.11%
	70	0.171	0.188	0.017	9.04%
	68	0.175	0.190	0.015	7.89%
	66	0.178	0.192	0.014	7.29%
	64	0.180	0.196	0.016	8.16%
	62	0.182	0.208	0.026	12.50%
	60	0.187	0.215	0.028	13.02%
	58	0.190	0.225	0.035	15.56%
	56	0.192	0.233	0.041	17.60%
	54	0.195	0.244	0.049	20.08%
	52	0.208	0.252	0.044	17.46%
	50	0.215	0.261	0.046	17.62%
	48	0.228	0.271	0.043	15.87%
	46	0.238	0.283	0.045	15.90%
	44	0.250	0.294	0.044	14.97%
	42	0.259	0.305	0.046	15.08%
	40	0.274	0.324	0.050	15.43%
	38	0.289	0.370	0.081	21.89%
	36	0.304	0.410	0.106	25.85%
	34	0.328	0.472	0.144	30.51%
	32	0.361	0.568	0.207	36.44%
	30	0.420	0.720	0.300	41.67%
Optimum Opint	29	0.520	1.200	0.680	56.67%
Zone II	30	0.780	1.250	0.470	37.60%
	32	1.070	1.362	0.292	21.44%
	34	1.256	1.477	0.221	14.96%
	36	1.380	1.562	0.182	11.65%
	38	1.501	1.650	0.149	9.03%
	40	1.605	1.736	0.131	7.55%